Predicting the $\sin\phi_S$ single-spin asymmetry of Λ production off a transversely polarized nucleon in SIDIS

Yongliang Yang,[1,*] Xiaoyu Wang,[2] and Zhun Lu[3,†]

[1]*College of Physics, Qingdao University, Qingdao 266071, China*
[2]*School of Physics and Microelectronics, Zhengzhou University, Zhengzhou 450001, China*
[3]*School of Physics, Southeast University, Nanjing 211189, China*

(Received 23 March 2021; accepted 17 May 2021; published 9 June 2021)

We investigate the transverse target spin asymmetry $A_{UT}^{\sin\phi_S}$ for the unpolarized Λ production in semi-inclusive deep inelastic scattering (SIDIS) with the transverse momentum of the final-state lambda hyperon being integrated out. The asymmetry is contributed by the product of the transversity distribution function $h_1(x)$ of the nucleon and the collinear twist-3 fragmentation function $\tilde{H}(z)$ of the Λ hyperon. The later one originates from the quark-gluon-quark correlation and is a naive time-reversal-odd function. We calculate $\tilde{H}$ of the Λ hyperon by adopting a diquark spectator model. Using the numerical result of $\tilde{H}(z)$ and the available parametrization of $h_1(x)$ from SIDIS data, we predict the $\sin\phi_S$ asymmetry in the electroproduction of the Λ hyperon in the kinematical region of Electron-Ion Collider (EIC), EIC in China (EicC), and COMPASS. In the phenomenological analysis, we include the evolution effect of the distribution functions and the fragmentation functions. The results show that the asymmetries for the Λ production SIDIS process are around 0.1 and may be accessible at EIC, EicC, and COMPASS. We also find that the evolution of fragmentation function can affect the size of asymmetry.

DOI: 10.1103/PhysRevD.103.114011

I. INTRODUCTION

Understanding the nonperturbative fragmentation mechanism in hard semi-inclusive processes is one of the important tasks in hadronic physics. Fruitful outcomes regarding fragmentation functions have been achieved by experimental measurements on e^+e^- annihilation [1–5], semi-inclusive deeply inelastic scattering (SIDIS) [6–9], and pp collision [10–15] as well as by theoretical studies [16–36]. Of particular interest are those related to the spin-orbit correlations, which are usually naive time-reversal odd (T odd). A renowned fragmentation function is the Collins function $H_1^\perp$ [16], which arises from the correlation between the transverse spin of the quark and the transverse momentum of the fragmented hadron. Another example is the Sivers-type fragmentation function $D_{1T}^\perp$ [22,37,38] reflecting the correlation between the transverse polarization of the final-state spin-1/2 hadron and the transverse momentum of the quark. Because these functions describe the asymmetric distribution of the hadron inside a fragmenting quark, they play important roles in the spin or azimuthal asymmetries in various high-energy processes [1–15]. Furthermore, these functions contain nontrivial QCD dynamics such as final-state interactions as well as the Wilson lines which ensure the gauge invariance of the operator definitions [39–44].

Recently, the twist-3 fragmentation functions arising from multiparton correlation [45–49] have also attracted a lot of attention. Particularly, a phenomenological study [50] on the inclusive pion production in single transversely polarized pp collision [12–15] shows that, besides the contribution from the twist-3 distribution $T_q(x,x)$ [51–54], the T-odd twist-3 fragmentation functions $\hat{H}$ and $\tilde{H}$ [55] should be included in the analysis in order to interpret the single spin asymmetry (SSA) in this process in a consistent way. The fragmentation function $\tilde{H}$ arising from quark-gluon-quark (qgq) correlation also contributes to the $\sin\phi_S$ asymmetry in SIDIS [56] through the combination $h_1(x) \otimes \tilde{H}(z)$, with $h_1(x)$ the tansversity distribution and ϕ_S the azimuthal angle of the transverse spin of the nucleon target. Thus, $\tilde{H}(z)$ provides a unique manner to probe the transversity of the proton via single-hadron production in the collinear framework. In Ref. [57], the fragmentation function of the pion meson was calculated by a quark-antiquark-spectator model. In Ref. [58], the SSA $A_{UT}^{\sin(\phi_S)}$ for the pion production at the Electron-Ion Collider (EIC) was predicted.

*yangyl@qdu.edu.cn
†zhunlu@seu.edu.cn

In this work, we will study the fragmentation function $\tilde{H}$ of the Λ hyperon as well as its role in the SSA of the $lp^{\uparrow} \to l'\Lambda X$ process. As the Λ hyperon contains the up, down, and strange valence flavors, which is more complicated than the pion meson, the study of the Λ fragmentation function will provide complimentary information on the hadronization mechanism involving spin-orbit correlation. The investigation could also obtain the flavor dependence [21] of the fragmentation process. For this purpose, we calculate $\tilde{H}$ of the Λ hyperon for the up, down, and strange quarks using a diquark spectator model. Previously, the model was applied to calculate the fragmentation function $D_{1T}^{\perp}$ and Collins functions of the Λ hyperon in Refs. [59,60]. In these cases, the spectator system is diquark, and the contributions from both the scalar diquark and vector diquark are taken into account. We also consider the gluon rescattering effect for the qgq correlation functions in the calculation. Based on the model results, we predict the $\sin\phi_S$ asymmetry in the $lp^{\uparrow} \to l'\Lambda X$ process, which can be measured by the COMPASS as well as the proposed EIC and the EIC in China (EicC). As these facilities cover different kinematical regions, it is necessary to consider the QCD evolution effect of $\tilde{H}$ to compare the result at different energy scales.

The remaining content of the paper is organized as follows. In Sec. II, we perform the calculation for twist-3 qgq fragmentation function $\tilde{H}$ by adopting the diquark spectator model and study the evolution effects of $\tilde{H}$. In Sec. III, we set up the formalism of the $\sin\phi_S$ asymmetry in SIDIS process with the transverse momentum of the final-state hadron being integrated. We present the numerical results of the $\sin\phi_S$ asymmetry in the electroproduction of the Λ hyperon at EIC, EicC, and COMPASS, using the formalism of the $\sin\phi_S$ asymmetry in a collinear framework. In Sec. IV, we summarize the results of the paper and give some conclusion.

II. MODEL CALCULATION OF FRAGMENTATION FUNCTION IN QGQ CORRELATOR

In this section, we present the model calculation of the twist-3 transverse momentum dependent fragmentation function $\tilde{H}(z, k_T)$ utilizing the diquark spectator model. The fragmentation function can be obtained from the trace of the transverse correlator $\tilde{\Delta}_A^{\alpha}(z, k_T)$

$$\frac{z}{4M_\Lambda}\mathrm{Tr}[(\tilde{\Delta}_{A\alpha}(z,k_T;S_\Lambda)+\tilde{\Delta}_{A\alpha}(z,k_T;-S_\Lambda))\sigma^{\alpha-}] = \tilde{H}(z,k_T)+i\tilde{E}(z,k_T), \tag{1}$$

where M_Λ is the mass of Λ hyperon, and the twist-3 qgq fragmentation correlator $\tilde{\Delta}_{A\alpha}$ can be expressed as [56,61]

$$\tilde{\Delta}_A^{\alpha}(z,k_T;S_\Lambda) = \sum_X \frac{1}{2z}\int \frac{d\xi^+ d^2\boldsymbol{\xi}_T}{(2\pi)^3}\int e^{ik\cdot\xi}\langle 0|\int_{\pm\infty^+}^{\xi^+} d\eta^+ \mathcal{U}^{\boldsymbol{\xi}_T}_{(\infty^+,\eta^+)} \times gF_\perp^{-\alpha}(\eta)\mathcal{U}^{\boldsymbol{\xi}_T}_{(\eta^+,\xi^+)}\psi(\xi)|P_\Lambda,S_\Lambda;X\rangle\langle P_\Lambda,S_\Lambda;X|\bar{\psi}(0)\mathcal{U}^{\mathbf{0}_T}_{(0^+,\infty^+)}\mathcal{U}^{\infty^+}_{(\mathbf{0}_T,\boldsymbol{\xi}_T)}|0\rangle\Big|_{\substack{\eta^+=\xi^+=0\\ \eta_T=\xi_T}} \tag{2}$$

with $\mathcal{U}^c_{(a,b)}$ the Wilson line (gauge link) running along the direction from a to b at the fixed position c. Detailed discussion on the Wilson line $\mathcal{U}$ has been given in Refs. [29,56,62,63]. The gauge invariant of correlator is guaranteed by the antisymmetric field strength tensor $F^{\mu\nu}$ of the gluon. The state $|P_\Lambda, S_\Lambda\rangle$ represents the final-state lambda hyperon with the momentum of P_Λ and the spin of S_Λ. In the diquark spectator model [64,65], the fragmentation function $\tilde{H}$ can be calculated from Fig. 1, where the contribution to the T-odd fragmentation function also originates from the imaginary part of the one-loop diagram [57,66]. Specifically, the quark-diquark-hyperon vertex $\langle P_\Lambda, S_\Lambda; X|\bar{\psi}(0)|0\rangle$ appearing in the rhs of Eq. (2) has the form

$$\langle P_\Lambda,S_\Lambda;X|\bar{\psi}(0)|0\rangle = \begin{cases} \bar{U}(P_\Lambda,S_\Lambda)\Upsilon_s\frac{i}{k-m_q} & \text{scalar diquark,}\\ \bar{U}(P_\Lambda,S_\Lambda)\Upsilon_v^{\mu}\frac{i}{k-m_q}\varepsilon_\mu & \text{axial-vector diquark,}\end{cases} \tag{3}$$

where k denotes the parent quark momentum and ε_μ is the polarization vector of the axial-vector diquark. The summation over all polarizations states of the axial-vector diquark can be expressed as $d_{\mu\nu} = \sum_\lambda \varepsilon_\mu^{*(\lambda)}\varepsilon_\nu^{(\lambda)}$, which has the form as $d_{\mu\nu} = -g_{\mu\nu} + \frac{P_{\Lambda\mu}P_{\Lambda\nu}}{M_\Lambda^2}$ [65]. The scalar and axial-vector coupling vertex of the quark-diquark-hyperon can be expressed by $\Upsilon_s = g_s(k^2)$ and $\Upsilon_v^{\mu} = \frac{g_v(k^2)}{\sqrt{3}}\gamma_5(\gamma^{\mu} + \frac{P_\Lambda^{\mu}}{M_\Lambda})$,

respectively. In this work, we assume that g_s and g_v have the same form $g_s = g_v = g_{qh}$ as Gaussian form denoted as g_{qh}

$$g_{qh}(k^2) \mapsto \frac{g_D}{z} e^{-\frac{k^2}{\Lambda^2}}, \tag{4}$$

where Λ^2 has the general form $\Lambda^2 = \lambda^2 z^\alpha (1-z)^\beta$ and g_D, λ, α, and β are the model parameters.

Analogously, we also provide the expression for the vertex $\langle 0|gF_\perp^{-\alpha}(\eta)\psi(\xi)|P_\Lambda, S_\Lambda; X\rangle$ in Eq. (2), in which the Feynman rules corresponding to the gluon field strength tensor $F^{\alpha\beta}$ are given by the factor $i(l^\alpha g_T^{\rho\beta} - l_T^\alpha g^{\beta\rho})$, as denoted by the open circle in Fig. 1 [57]. With the above Feynman rules, the contribution of Fig. 1 to the correlator $\tilde{\Delta}_A^\alpha$ is given by

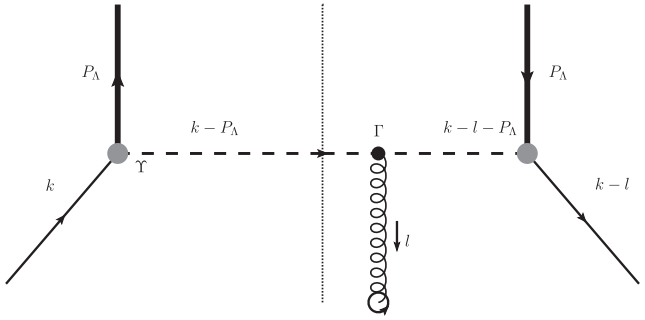

FIG. 1. The Feynman diagram that is relevant to the calculation of the quark-gluon-quark correlator in the diquark model. The notations Υ and Γ describe quark-diquark-hyperon and gluon-diquark coupling vertices, respectively.

$$\tilde{\Delta}_{As}^\alpha(z, k_T, S_\Lambda) = -i\frac{C_F\alpha_S}{2(2\pi)^2(1-z)P_\Lambda^-}\frac{1}{k^2-m^2}\int\frac{d^4l}{(2\pi)^4} \times \frac{(l^- g_T^{\alpha\rho} - l^\alpha n_+^\rho)(\not{k} - \not{l} + m)\bar{\Upsilon}_s U(P_\Lambda, S_\Lambda)\bar{U}(P_\Lambda, S_\Lambda)\Upsilon_s(\not{k}+m)}{((k-l)^2-m^2)(l^2-i\epsilon)((k-l-P_\Lambda)^2-m_s^2)(-l^- - i\epsilon)}\bar{\Gamma}_\rho \tag{5}$$

$$\tilde{\Delta}_{Av}^\alpha(z, k_T, S_\Lambda) = i\frac{C_F\alpha_S}{2(2\pi)^2(1-z)P_\Lambda^-}\frac{1}{k^2-m^2}\int\frac{d^4l}{(2\pi)^4} \times \frac{(l^- g_T^{\alpha\rho} - l^\alpha n_+^\rho)(\not{k} - \not{l} + m)\bar{\Upsilon}_v^\nu U(P_\Lambda, S_\Lambda)\bar{U}(P_\Lambda, S_\Lambda)\Upsilon_v^\mu(\not{k}+m)}{((k-l)^2-m^2)(l^2-i\epsilon)((k-l-P_\Lambda)^2-m_s^2)(-l^- - i\epsilon)} d^{i\mu}d^{j\nu}\bar{\Gamma}_{ij\rho}, \tag{6}$$

where $\tilde{\Delta}_{As}^\alpha$ and $\tilde{\Delta}_{Av}^\alpha$ represent scalar and axial-vector diquark forms of qgq correlator, respectively. Here, the light-cone coordinates $a^\pm = a\cdot n_\pm = (a^0 \pm a^3)/\sqrt{2}$ are applied, and $k^- = P_\Lambda^-/z$. In Fig. 1, the notation Γ describes the gluon-diquark coupling vertex. To explicitly calculate the correlator, we choose the form for the vertex between the gluon and the scalar diquark (Γ_s) and the axial-vector diquark (Γ_v),

$$\Gamma_s^{\rho,a} = iT^a(2k - 2P - l)^\rho \tag{7}$$

$$\Gamma_v^{\rho\mu\nu,a} = -iT^a[(2k-2P-l)^\rho g^{\mu\nu} - (k-P-l)^\mu g^{\nu\rho} - (k-P)^\nu g^{\rho\mu}], \tag{8}$$

where T^a is the Gell-Mann matrix.

Similar to the calculation of the T-odd quark-gluon-quark fragmentation function $\tilde{G}^\perp$ in Ref. [66], we obtain the imaginary part of the correlator using the Cutkosky cut rules to put the gluon and quark lines on the mass shell. This corresponds to the following replacements on the propagators by using the Dirac delta functions:

$$\frac{1}{l^2 + i\varepsilon} \to -2\pi i\delta(l^2),$$
$$\frac{1}{(k-l)^2 - m^2 + i\varepsilon} \to -2\pi i\delta((k-l)^2 - m^2). \tag{9}$$

Using the cut rules in Eq. (9), we perform the trace and integration over the loop momentum l; we first give the scalar diquark component of $\tilde{H}(z, k_T^2)$ for the Λ hyperon as

$$\tilde{H}^s(z, \boldsymbol{k}_T^2) = \frac{\alpha_S g_{qh}^2 C_F}{(2\pi)^4 M_\Lambda(1-z)}\frac{1}{k^2-m^2}\tilde{H}_{1s}(z, \boldsymbol{k}_T^2), \tag{10}$$

where

$$\tilde{H}_{1s}(z, \boldsymbol{k}_T^2) = \frac{1}{z}[z\mathcal{A}(z^2\boldsymbol{k}_T^2 m + k^2(z-1)(zm + M_\Lambda)) + \mathcal{B}M_\Lambda(z(z-1)mM_\Lambda - z^2\boldsymbol{k}_T^2 + (z-1)M_\Lambda^2)]. \tag{11}$$

Here, $k^2 = z\boldsymbol{k}_T^2/(1-z) + m_s^2/(1-z) + m_h^2/z$.

Similarly, using the gluon-diquark vertex given in Eq. (8), we can also calculate the expression for $\tilde{H}$ from the axial vector diquark component

$$\tilde{H}^v(z,k_T^2)=\frac{\alpha_S g_{qh}^2 C_F}{4(2\pi)^4 M_\Lambda(1-z)}\frac{1}{k^2-m^2}(\tilde{H}_s^v(z,\boldsymbol{k}_T^2)+\tilde{H}_0^v(z,\boldsymbol{k}_T^2)+\tilde{H}_1^v(z,\boldsymbol{k}_T^2)+\tilde{H}_2^v(z,\boldsymbol{k}_T^2)), \tag{12}$$

where the four terms in the rhs of Eq. (12) are given by

$$\tilde{H}_s^v=\frac{4}{z}[(z\mathcal{A}(z^2\boldsymbol{k}_T^2 m+k^2(z-1)(zm+M_\Lambda))+\mathcal{B}M_\Lambda(z(z-1)mM_\Lambda-z^2\boldsymbol{k}_T^2+(z-1)M_\Lambda^2)], \tag{13}$$

$$\tilde{H}_0=-2z\frac{\boldsymbol{k}_T^2}{3M_\Lambda}[(2\mathcal{C}\mathcal{C}k^-k\cdot P+2\mathcal{C}\mathcal{D}k^-M_\Lambda^2+2z\mathcal{C}\mathcal{E}k^-k^--\mathcal{C}k^-k^2z+\mathcal{C}k^-m^2z)], \tag{14}$$

$$\begin{aligned}\tilde{H}_1=&\frac{2}{3M_\Lambda^2 z}\{zk\cdot P[z(\boldsymbol{k}_T^2(\mathcal{A}\mathcal{A}mz-2\mathcal{A}(mz+M_\Lambda))+\mathcal{A}\mathcal{A}k^2(mz+M_\Lambda)\\&-2\mathcal{A}k^2mz-5\mathcal{A}k^2M_\Lambda-3\mathcal{A}m^2M_\Lambda-2\mathcal{B}mM_\Lambda^2)+\mathcal{A}\mathcal{B}M_\Lambda^2(mz-3M_\Lambda)]\\&-2m_h z(\mathcal{A}\mathcal{A}-2\mathcal{A})(k\cdot P)^2+M_\Lambda[z(M_\Lambda(\mathcal{A}\mathcal{B}k^2mz^2+\mathcal{A}\mathcal{B}k^2M_\Lambda z+\mathcal{B}\mathcal{B}M_\Lambda^2(mz-M_\Lambda)\\&-2\boldsymbol{I}_2(k^2-m^2)(mz+M_\Lambda)+m\mathcal{W}_1 z-M_\Lambda\mathcal{W}_1)+\boldsymbol{k}_T^2(\mathcal{A}\mathcal{B}mM_\Lambda z^2+\mathcal{A}(z^2(k^2+m^2)-4M_\Lambda^2))\\&+\mathcal{A}k^2(z^2(k^2+m^2)+4mM_\Lambda z+4M_\Lambda^2))+2\mathcal{B}M_\Lambda^2(-z^2(\boldsymbol{k}_T^2+m^2)+2mM_\Lambda z+2M_\Lambda^2)]\},\end{aligned} \tag{15}$$

$$\begin{aligned}\tilde{H}_2=&\frac{4}{3M_\Lambda}[M_\Lambda(\mathcal{A}+\mathcal{B}z)(M_\Lambda(2\boldsymbol{k}_T^2+k^2+m^2)+2mk\cdot P)-(k\cdot P+mM_\Lambda)((\mathcal{A}\mathcal{A}+\mathcal{A}\mathcal{B}z)k\cdot P\\&+(\mathcal{A}\mathcal{B}+z\mathcal{B}\mathcal{B})M_\Lambda^2+z\mathcal{W}_1))].\end{aligned} \tag{16}$$

Here, the number of the subscript for $\tilde{H}$ denotes the number of the factor l^- in the numerator of Eq. (1) after the trace calculation is performed. $\mathcal{A}$, $\mathcal{B}$, $\mathcal{C}$, and $\boldsymbol{I}_2$ are functions of k^2, m, m_D, and M_Λ and can be found in Ref. [59]. The functions $\mathcal{A}\mathcal{A}$, $\mathcal{A}\mathcal{B}$, $\mathcal{B}\mathcal{B}$, $\mathcal{C}\mathcal{C}$, $\mathcal{C}\mathcal{D}$, $\mathcal{C}\mathcal{E}$, and $\mathcal{W}_1$ come from the following double-l integrals:

$$\int d^4l\frac{l^\mu l^\nu\delta(l^2)\delta((k-l)^2-m^2)}{((k-P_h-l)^2-m_s^2)}=\mathcal{A}\mathcal{A}k^\mu k^\nu+\mathcal{B}\mathcal{B}P^\mu P^\nu+\mathcal{A}\mathcal{B}(k^\mu P^\nu+P^\mu k^\nu)+g^{\mu\nu}\mathcal{W}_1, \tag{17}$$

$$\begin{aligned}\int d^4l\frac{l^\mu l^\nu\delta(l^2)\delta((k-l)^2-m^2)}{((k-P_h-l)^2-m_s^2)(-l\cdot n_++i\epsilon)}=&\mathcal{C}\mathcal{C}_f k^\mu k^\nu+\mathcal{D}\mathcal{D}_f P^\mu P^\nu+\mathcal{E}\mathcal{E}_f n_+^\mu n_+^\nu\\&+\mathcal{C}\mathcal{D}_f(k^\mu P^\nu+P^\mu k^\nu)+\mathcal{C}\mathcal{E}_f(k^\mu n_+^\nu+n_+^\mu k^\nu)+\mathcal{D}\mathcal{E}_f(n_+^\mu P^\nu+P^\mu n_+^\nu)+g^{\mu\nu}\mathcal{W}_2.\end{aligned} \tag{18}$$

Note that a main difference between the calculation for the Λ hyperon and the one for the pion [57] is that there are double l's in the numerators in Eqs. (17) and (18), which need to be evaluated carefully. We provide the complete expressions for these functions in the Appendix.

We will focus on the favored quark contribution to the fragmentation function of Λ, i.e., $u\to\Lambda$ or $s\to\Lambda$, while the unfavored quark contribution is zero. Assuming an SU(6) spin-flavor symmetry, the fragmentation functions of the Λ hyperon for light flavors satisfy the relations between different quark flavors and diquark types [67,68]

$$D^{u\to\Lambda}=D^{d\to\Lambda}=\frac{1}{4}D^{(s)}+\frac{3}{4}D^{(v)},\quad D^{s\to\Lambda}=D^{(s)}, \tag{19}$$

where u, d, and s denote the up, down, and strange quarks, respectively. In this study, we assume that the relation in Eq. (19) holds for all fragmentation functions. Neglecting the mass differences between the up, down, and strange quarks ($m=0.36$ GeV), we obtain the light flavors fragmentation function $\tilde{H}$ as

$$\tilde{H}^{u\to\Lambda}=\tilde{H}^{d\to\Lambda}=\frac{1}{4}\tilde{H}^{(s)}+\frac{3}{4}\tilde{H}^{(v)},\quad \tilde{H}^{s\to\Lambda}=\tilde{H}^{(s)}, \tag{20}$$

To obtain the numerical result for $\tilde{H}$, we should choose the values of the parameters

$$\begin{aligned}&g_D=1.983^{+0.119}_{-0.111},\qquad m_D=0.745^{+0.03}_{-0.028}\ \text{GeV},\\&\lambda=5.967^{+0.274}_{-0.26}\ \text{GeV},\qquad \alpha=0.5(\text{fixed}),\\&\beta=0(\text{fixed}),\end{aligned} \tag{21}$$

were obtained by fitting the model result of D_1 in the same model to the de Florian-Stratmann-Vogelsang (DSV) parametrization for D_1 at the model scale $Q^2 = 0.23\ \mathrm{GeV}^2$. The choice of this scale is consistent with the starting scale of the "radiative parton model," which has proven phenomenologically successful in the analysis of the unpolarized/polarized parton densities [69,70] and photon fragmentation functions [71,72].

Using the model parameters, we calculate the collinear twist-3 fragmentation function $\tilde{H}(z)$ of Λ by integrating over the transverse momentum:

$$\tilde{H}(z) = z^2 \int d^2\boldsymbol{k_T} \tilde{H}(z, \boldsymbol{k_T^2}). \tag{22}$$

Since the energy scale in the experiments covers a wide range of Q, which is much higher than the model scale, it is necessary to include the QCD evolution effects of the fragmentation functions. There are studies on the evolution of several twist-3 fragmentation functions in the literature [32,33,47,73]. However, the DGLAP evolution kernel for $\tilde{H}$ is still unknown. In this work, we assume the evolution kernel of $\tilde{H}$ is the same as the homogenous terms in the kernel of $\hat{H}^{(3)}(z)$ in Ref. [33], as has been done in Ref. [74]. This kernel has the same form as that of the transversity distribution function. In Ref. [58], the evolution kernel for the pion $\tilde{H}(z)$ has also been adopted as the same as that for the transversity distribution function h_1, which was motivated by the fact that $\tilde{H}$ is also a chiral odd fragmentation function. To do this, we apply the QCDNUM package [75] and customize the package to include the kernel of transversity to perform the evolution.

In the left and right panels of Fig. 2, we plot the z dependence of the collinear twist-3 fragmentation function $z\tilde{H}(z)$ of Λ for s and $u(d)$ quark of the twist-3 fragmentation functions at the model scale $Q^2 = 0.23\ \mathrm{GeV}^2$ (the solid lines) and the evolved results at $Q^2 = 100\ \mathrm{GeV}^2$ (the dotted lines), respectively. The shaded areas correspond to the uncertainty bands due to the uncertainties of the model parameters. Figure 2 shows that the magnitude of $z\tilde{H}(z)$ for $u(d) \to \Lambda$ increases with increasing z when $0 < z < 0.9$, while it decreases with increasing z after $z > 0.9$ at the model scale, while the peak is around $z = 0.5$ for the s quark. The evolved fragmentation functions at $Q^2 = 100\ \mathrm{GeV}^2$ show the relatively strong impact of the evolution effects. The z dependences of the $u(d)$ and s quark for $z\tilde{H}$ are obviously different in the entire z region. We can see that the evolution from low Q to higher Q increases the sizes of $u(d) \to \Lambda$ in the region $z < 0.4$, while the region for the strange quark is $z < 0.25$. This is because the s quark only comes from the contribution of the scalar diquark component in Eq. (20).

III. PREDICTION ON THE $\sin\phi_S$ TRANSVERSE SSAS OF Λ HYPERON PRODUCTION IN SIDIS

The process under study is the unpolarized Λ production in the SIDIS process with an unpolarized lepton beam colliding on a transversely polarized nucleon beam (or target),

$$l(\ell) + N^{\uparrow}(P) \to l(\ell') + \Lambda(P_\Lambda) + X(P_X), \tag{23}$$

where l and l' stand for the momenta of the incoming and outgoing leptons and P and P_Λ denote the momenta of the target nucleon and the final-state Λ hyperon, respectively. The momentum of the exchanged virtual photon is defined as $q = l - l'$ and $Q^2 = -q^2$. The reference frame in this work was adopted as in Fig. 3, in which we will consider the case the polarization of the detected Λ hyperon is not measured. The azimuthal angle ϕ_S stands for the angle between the lepton scattering plane and the direction of the transverse spin of the nucleon target.

We introduce the invariant variables to express the differential cross section as [56]

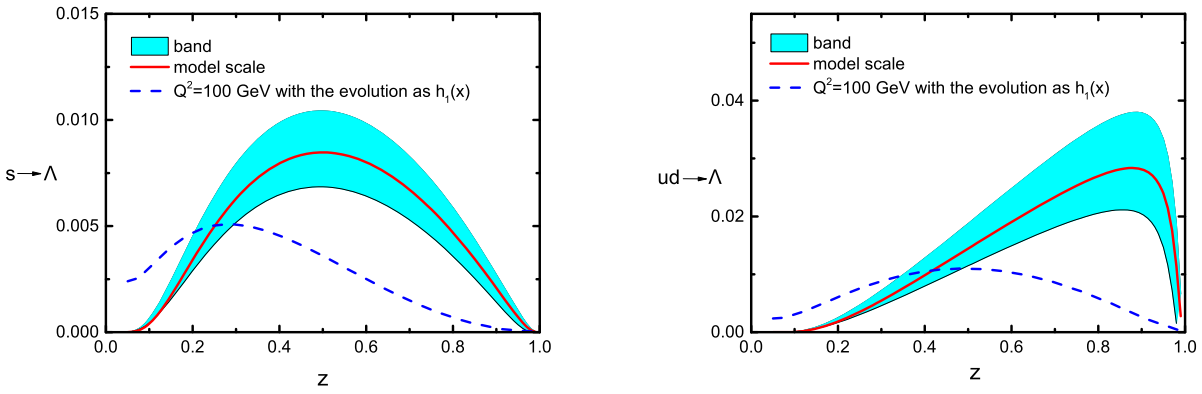

FIG. 2. Result of $z\tilde{H}^{\Lambda/s}(z)$ (left panel) and $z\tilde{H}^{\Lambda/u(d)}(z)$ (right panel) at the model scale $Q^2 = 0.23\ \mathrm{GeV}^2$ (red solid lines) and the evolved results at $Q^2 = 100\ \mathrm{GeV}^2$ (blue dashed lines). The shaded areas correspond to the uncertainty bands due to the uncertainties of the model parameters.

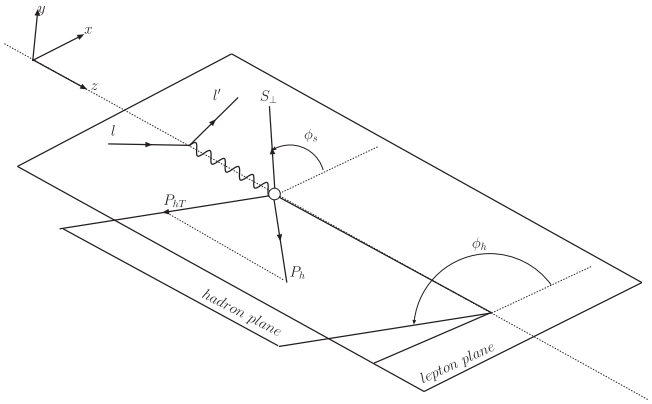

FIG. 3. The definition of the azimuthal angles in SIDIS. P_h stands for the momentum of the Λ hyperon hadron, $S_\perp$ is the transverse component of the spin vector S with respect to the virtual photon momentum [56].

$$x=\frac{Q^2}{2P\cdot q},\qquad y=\frac{P\cdot q}{P\cdot l},\qquad z=\frac{P\cdot P_h}{P\cdot q},$$
$$\gamma=\frac{2Mx}{Q},\qquad W^2=(P+q)^2,\qquad s=(P+l)^2,$$

where M denotes the mass of the target nucleon. With the invariant variables, the differential cross section of the process for unpolarized Λ production in SIDIS off an transverse polarized target can be expressed as [56,58]

$$\begin{aligned}\frac{d^6\sigma}{dxdydzd\phi_h d\phi_S dP_{hT}^2}&=\frac{\alpha^2}{xyQ^2}\frac{y^2}{2(1-\varepsilon)}\left(1+\frac{\gamma^2}{2x}\right)\\&\times\{F_{UU,L}(x,z,P_T)+|S_\perp|[\sin\phi_S F_{UT}^{\sin\phi_S}(x,z,P_T)\\&+\sin(2\phi_h-\phi_S)F_{UT}^{\sin(2\phi_h-\phi_S)}(x,z,P_T)\\&+\text{leading twist terms}]\},\end{aligned}\tag{24}$$

where ε is the ratio of the longitudinal and transverse photon flux

$$\varepsilon=\frac{1-y-\frac{1}{4}\gamma^2y^2}{1-y+\frac{1}{2}y^2+\frac{1}{4}\gamma^2y^2}.\tag{25}$$

After integrating over $\boldsymbol{P}_{hT}$, the differential cross section in Eq. (24) turns to the form

$$\begin{aligned}\frac{d^4\sigma}{dxdydzd\phi_S}&=\frac{2\alpha^2}{xyQ^2}\frac{y^2}{2(1-\varepsilon)}\left(1+\frac{\gamma^2}{2x}\right)\\&\times\{F_{UU,L}(x,z)+|S_\perp|\sqrt{2\varepsilon(1+\varepsilon)}\sin\phi_S F_{UT}^{\sin\phi_S}(x,z)\\&+\cdots\}.\end{aligned}\tag{26}$$

Here, the nonvanishing integrated structure functions are [56,76]

$$F_{UU}(x,z)=x\sum_q e_q^2 f_1^q(x)D_1^q(z),\tag{27}$$

$$F_{UT}^{\sin\phi_S}(x,z)=-x\sum_q e_q^2\frac{2M_\Lambda}{Q}h_1^q(x)\frac{\tilde{H}^q(z)}{z},\tag{28}$$

and only the convolution of the transversity and the twist-3 collinear fragmentation function $\tilde{H}$ remains in the structure function $F_{UT}^{\sin\phi_S}$.

One should note that there are more terms related to the twist-3 parton distribution functions (PDFs) or fragmentation function (FFs) [56] in the transverse momentum dependent structure function $F_{UT}^{\sin(\phi_S)}(x,z,P_T)$ than the collinear form in Eq. (28), where P_T is the transverse momentum of the final-state Λ. After integrating out $\boldsymbol{P}_T$, only the convolution of transversity and the T-odd twist-3 fragmentation function $\tilde{H}(z)$ survives, and all other terms drop out. To do this, the integration has to be performed in the whole region of transverse momentum P_{hT}, which may be challenging for experimental measurement.

Following Eqs. (27) and (28), we can obtain the z-dependent $\sin\phi_S$ asymmetry:

$$A_{UT}^{\sin\phi_s}(z)=\frac{\int dx\int dy\,\frac{\alpha^2}{xyQ^2}\frac{y^2}{2(1-\epsilon)}(1+\frac{\gamma^2}{2x})\sqrt{2\epsilon(1+\epsilon)}F_{UT}^{\sin\phi_s}(x,z)}{\int dx\int dy\,\frac{\alpha^2}{xyQ^2}\frac{y^2}{2(1-\epsilon)}(1+\frac{\gamma^2}{2x})F_{UU}(x,z)}.\tag{29}$$

In a similar way, x-dependent $\sin\phi_S$ asymmetry can be written as

$$A_{UT}^{\sin\phi_S}(x)=\frac{\int dy\int dz\,\frac{\alpha^2}{xyQ^2}\frac{y^2}{2(1-\epsilon)}(1+\frac{\gamma^2}{2x})\sqrt{2\epsilon(1+\epsilon)}F_{UT}^{\sin\phi_s}(x,z)}{\int dy\int dz\,\frac{\alpha^2}{xyQ^2}\frac{y^2}{2(1-\epsilon)}(1+\frac{\gamma^2}{2x})F_{UU}(x,z)},\tag{30}$$

To estimate the $\sin\phi_S$ asymmetry, we need the information of the transversity distribution $h_1^q(x)$, for which we adopt the parametrization from Ref. [31],

$$h_1^q(x)=\frac{1}{2}\mathcal{N}_q^T(x)[f_1^q(x)+g_1^q(x)],\tag{31}$$

with

$$\mathcal{N}_q^T(x)=N_q^T x^\alpha(1-\beta)^\beta\frac{(\alpha+\beta)^{\alpha+\beta}}{\alpha^\alpha\beta^\beta},\tag{32}$$

where values of the parameters $N_u^T=0.36$, $N_d^T=-1.00$, $\alpha=1.06$, and $\beta=3.66$ are taken from Ref. [31].

The parametrization for the unpolarized distribution $f_1^q(x)$ is from Ref. [77], and that for the helicity distribution $g_1^q(x)$ is from Ref. [78]. We note that currently there is no available parametrization on $h_1^q(x)$ for the sea quarks; therefore, in this calculation, we will not consider the contribution from the transversity of the sea quarks.

The kinematical region of the EIC adopted in our calculation is [79]

$$0.001 < x < 0.4, \quad 0.01 < y < 0.95, \quad 0.2 < z < 0.8,$$
$$Q^2 > 1\ \mathrm{GeV}^2, \quad \sqrt{s} = 45\ \mathrm{GeV}, \quad W > 5\ \mathrm{GeV}, \tag{33}$$

where W is invariant mass of the virtual photon-nucleon system and $W^2 \approx \frac{1-x}{x} Q^2$. As for the EicC, we adopt the following kinematical cuts [80,81]:

$$0.005 < x < 0.5, \quad 0.07 < y < 0.9, \quad 0.2 < z < 0.7,$$
$$Q^2 > 1\ \mathrm{GeV}^2, \quad \sqrt{s} = 16.7\ \mathrm{GeV}, \quad W > 2\ \mathrm{GeV}. \tag{34}$$

As the kinematics at EIC and EicC cover a wide range of Q, the QCD evolution effect of the distribution and fragmentation functions are also considered.

The numerical results of the $\sin\phi_S$ asymmetries for Λ hyperon production at EIC and EicC are shown in Figs. 4 and 5, respectively. The left panel and the right panel plot the asymmetries as functions of x and z. The dashed lines depict the results simultaneously evolving the fragmentation function $\tilde{H}$ and distribution function $h_1(x)$. The solid lines denote the asymmetries without considering the evolution of the fragmentation functions $\tilde{H}$. We find that the $\sin\phi_S$ asymmetries for the Λ hyperon production are negative. The magnitude of the asymmetry at EIC and EicC is around 0.1, which is quite sizable. We also find that the x-dependent asymmetries have a peak at the intermediate x region, around $x \approx 0.2$, and the magnitude of the z-dependent asymmetry increases with increasing z. Comparing our results with the same $\sin\phi_S$ asymmetry in pion production [58], we find that the signs of asymmetry are both are negative; However, the magnitude of the asymmetry in Λ production is several times larger than the one in pion production. The difference may

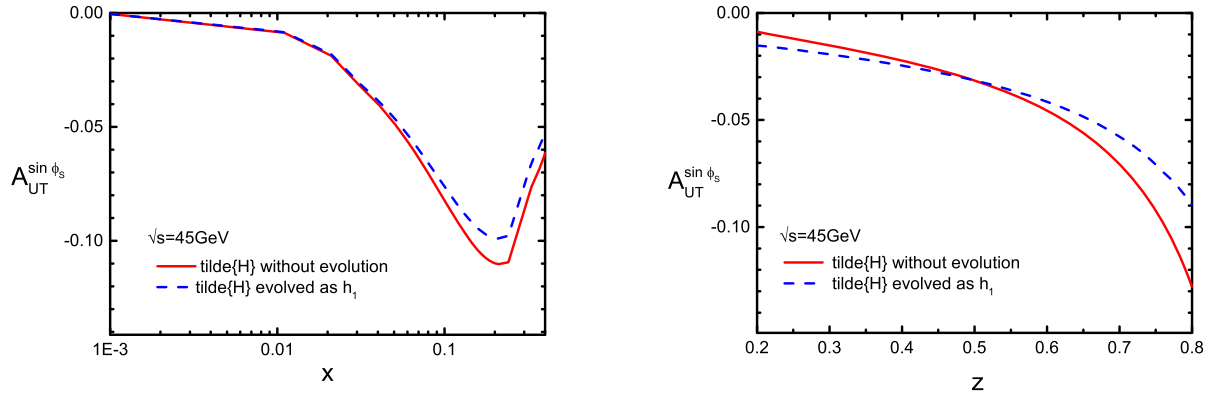

FIG. 4. Transverse SSA $A_{UT}^{\sin\phi_S}$ of Λ hyperon production in SIDIS at EIC for $\sqrt{s} = 45$ GeV. The left and the right panels show the x-dependent and the z-dependent asymmetries, respectively.

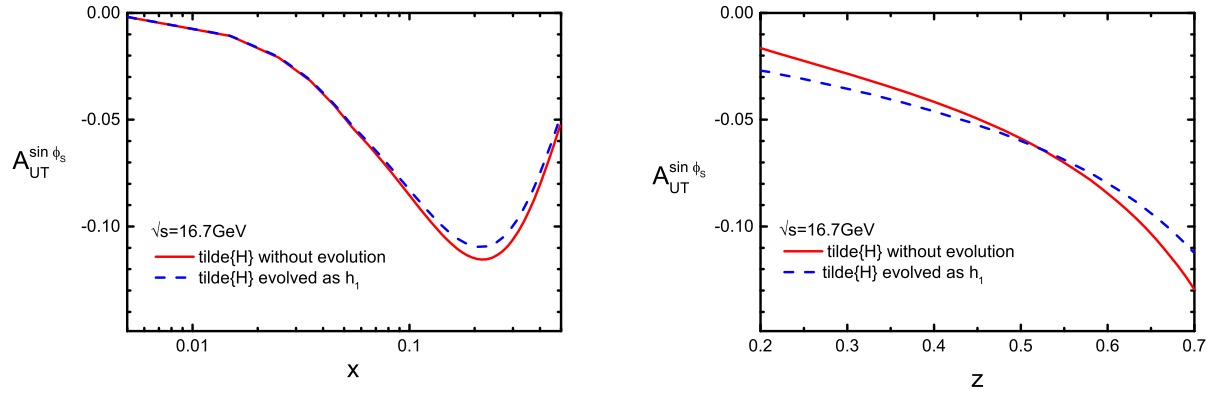

FIG. 5. Transverse SSA $A_{UT}^{\sin\phi_S}$ of Λ hyperon production in SIDIS at EicC for $\sqrt{s} = 16.7$ GeV. The left and the right panels show the x-dependent and the z-dependent asymmetries, respectively.

be caused by the factor $\frac{M_h}{Q}$ appearing in Eq. (28) as M_Λ is almost 1 order of magnitude larger than M_π. Therefore, there could be a great opportunity to measure the $\sin\phi_S$ asymmetry in Λ production at a future EIC and EicC.

Another important observation is that the evolution effect for the $\sin\phi_S$ asymmetry is substantial in a certain kinematical region at both the EIC and EicC. First of all, as shown by the dashed lines in Figs. 4 and 5, the magnitudes of the x-dependent and z-dependent asymmetries for Λ hyperon have changed substantially by the QCD evolution effect. Second, in the small-x region ($x < 0.04$ at EIC) and ($x < 0.07$ at EicC), the evolution does not affect the x-dependent asymmetries, while the evolution effect is sizable in the intermediate-x region. For the z-dependence asymmetries, the evolution effect may be observed in the all z region, where the evolution effect of size is smaller than nonevolution result in the region $z > 0.5$ at EIC and EicC; thereby, it should not be neglected. Nevertheless, the evolution almost does not change the signs and the shapes of the asymmetries.

Finally, we estimate the transverse asymmetries for Λ at COMPASS, which applies a 160 GeV muon beam scattering off the nucleon target. In this calculation, we adopt the following kinematical cuts [82]:

$$Q^2 > 1\ \mathrm{GeV}^2, \quad 0.004 < x < 0.7, \quad 0.1 < y < 0.9, \quad z > 0.2, \quad W > 5\ \mathrm{GeV}, \quad E_h > 1.5\ \mathrm{GeV}. \tag{35}$$

The results of the x- and z-dependent asymmetries are depicted in the left panel and right panels in Fig. 6, respectively. The solid lines denote the asymmetries without considering the evolution of fragmentation functions $\tilde{H}$ in Eqs. (30) and (29). The dashed lines correspond to the evolution of $\tilde{H}^q(z)$ as h_1. We find that the overall tendency of the asymmetries at the COMPASS are similar to that at the EIC and EicC. The evolution effect for x-dependent asymmetry may be observed in the region $x > 0.05$, and z-dependent asymmetry is larger than that of the EIC and EicC.

In Figs. 7–9, we also plot the Q^2 dependence of the asymmetry $A_{UT}^{\sin\phi_S}$ at fixed $x = 0.4$ at different facilities (EIC, EicC, and COMPASS). The left and right panels correspond to the asymmetries at $z = 0.4$ and $z = 0.6$,

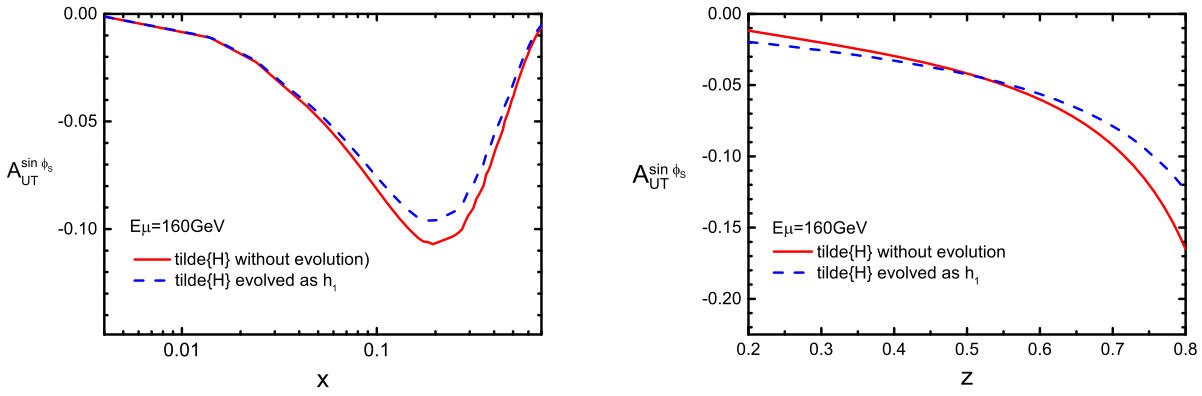

FIG. 6. Transverse SSA $A_{UT}^{\sin\phi_S}$ of Λ hyperon production in SIDIS at COMPASS for $E_\mu = 160$ GeV. The left and the right panels show the x-dependent and the z-dependent asymmetry, respectively.

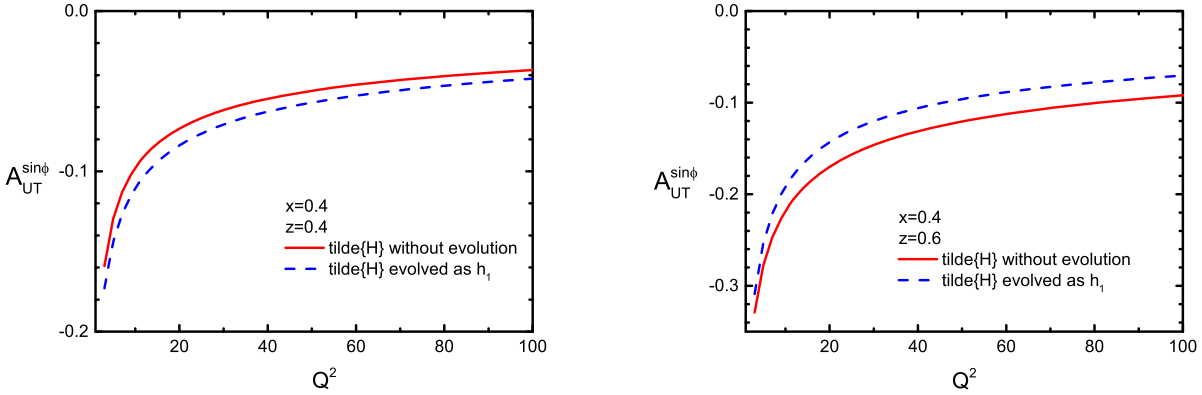

FIG. 7. Q^2 dependence of the transverse SSA $A_{UT}^{\sin\phi_S}$ at EIC with evolution (dashed lines) and without evolution (solid lines). The left and the right panels show the numerical results at $x = 0.4$, $z = 0.4$ and $x = 0.4$, $z = 0.6$, respectively.

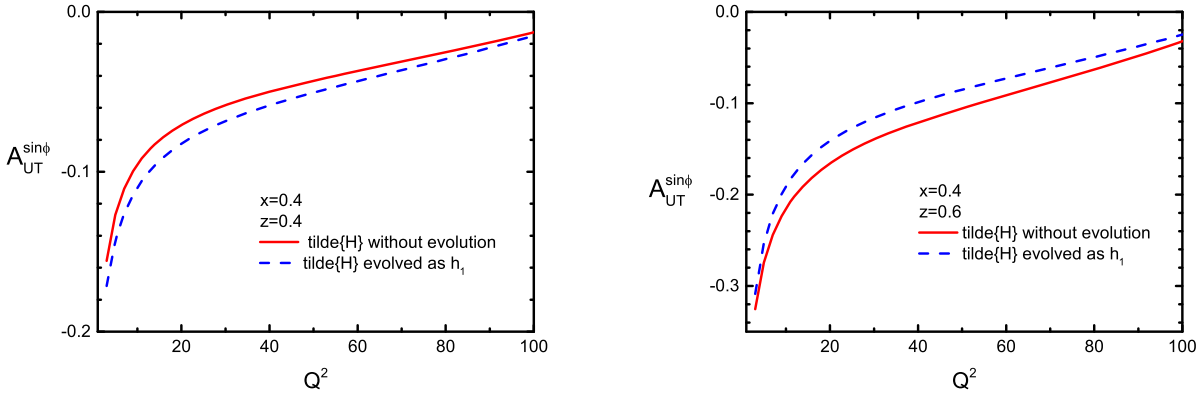

FIG. 8. Q^2 dependence of the transverse SSA $A_{UT}^{\sin\phi_S}$ at EicC with evolution (dashed lines) and without evolution (solid lines). The left and the right panels show the numerical results at $x = 0.4$, $z = 0.4$ and $x = 0.4$, $z = 0.6$, respectively.

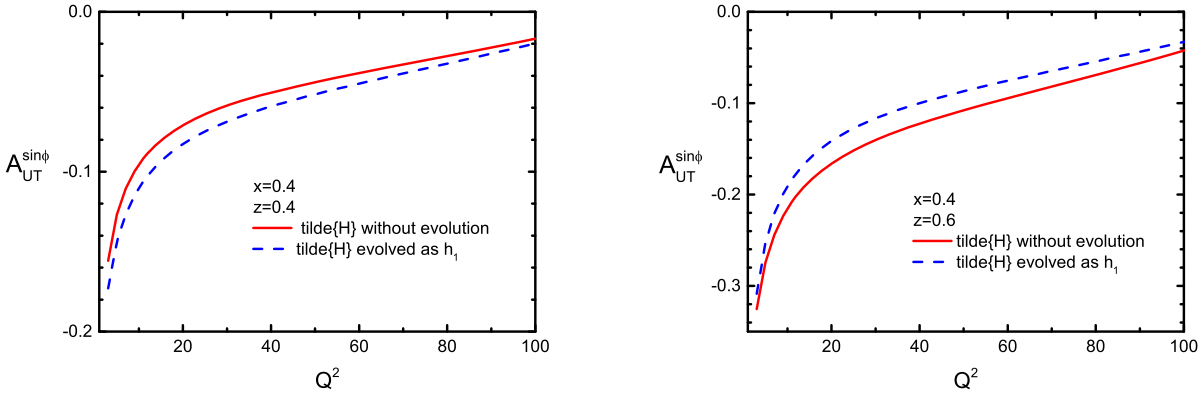

FIG. 9. Q^2 dependence of the transverse SSA $A_{UT}^{\sin\phi_S}$ at COMPASS with evolution (dashed lines) and without evolution (solid lines). The left and the right panels show the numerical results at $x = 0.4$, $z = 0.4$ and $x = 0.4$, $z = 0.6$, respectively.

respectively. Similarly to Fig. 4, the dashed lines depict the results simultaneously evolving the fragmentation function $\tilde{H}$ and transversity function; the solid lines denote the asymmetries without the evolution for $\tilde{H}$. At $x = 0.4$, $z = 0.4$, the asymmetry with evolution is larger than that without evolution, while at $x = 0.4$, $z = 0.6$, the two results are reversed. Moreover, the Q^2-dependent asymmetry decreases fast with increasing Q^2. One should note that the main reason of this decreasing is the twist-3 nature of the $\sin\phi_S$ asymmetry; that is, it is suppressed by a factor of $1/Q$. Including the evolution of $\tilde{H}$ will not change this tendency. Nevertheless, there is still a quantitative impact on the size of the asymmetry due to evolution, as can be seen from the difference between the asymmetry with evolution and that without evolution.

Some comments are in order. First, in the model calculation, we have calculated not only the $\tilde{H}^{\Lambda/q}$ for the up and down quarks but also that for the strange quark, while in the phenomenological analysis of the $\sin\phi_S$ asymmetry, we only have only considered the contributions from the up and down quarks. This is because currently there is no available information for the transversity of the sea quarks. In several phenomenological studies [83,84], the transversity of the sea quarks were included in the calculation through model assumptions, such as assuming the sea quark transversity is proportional to that of the valence quarks. In this work, we refrain from doing so since at this stage our result is a rough estimate of the asymmetry. The $\tilde{H}^{\Lambda/s}$ could be measurable, provided the transversity of the strange quark is sizable. Second, in this work, we consider the Λ production in SIDIS process, which is normally more difficult to measure than the meson production. However, in this process, it is not necessary to measure the polarization of the Λ. Besides, as our estimate indicates, the asymmetry is quite sizable at EIC, EicC, and COPMASS due to the fact that M_Λ/Q is much larger than M_π/Q. Thus, we expect that the $\sin\phi_S$ asymmetry of Λ production in SIDIS can be measured with the help of high statistics of the future ep facilities. Third, in our model, we assume that the scalar and axial-vector diquark couplings have the same form. It has the advantage of keeping the SU(3) flavor symmetry and corresponding to the DSV parametrization [18], where all the light flavors fragment equally into Λ hyperon. SU(3) flavors symmetry breaking

may alter the asymmetry quantitatively, and we expect that they will not change our results qualitatively. Finally, in our work the DGLAP evolution kernel is chosen as the same as the leading-order splitting kernel for transversity h_1; the only nonzero splitting kernel is $\Delta_T P_{qq}$. Therefore, unfavored FFs remains zero via evolution starting from zero input at the initial scale. To generate nonzero unfavored FFs through evolution, the next-to-leading-order evolution kernel has to be included, which is beyond the scope of our paper.

IV. CONCLUSION

In this work, we have studied the single-spin $\sin\phi_S$ asymmetry of the Λ production in SIDIS off an transversely polarized proton target. Since the transverse momentum dependent (TMD) version of this asymmetry contains many terms, it is necessary to integrate out P_T to relate the asymmetry to the convolution of transversity and the T-odd twist-3 function $\tilde{H}(z)$. However, in practice, it may be challenging for experimental measurement to cover the entire P_T region. Thus, model predictions could be very useful for acquiring the knowledge of the $\sin\phi_S$ asymmetry in the case P_T is integrated out. We have calculated the twist-3 T-odd quark-gluon-quark fragmentation function $\tilde{H}$ of the Λ hyperon with two different types of the diquark spectator model by considering both scalar and axial-vector diquarks [65,85]. The relation between the quark flavors and diquark types for the fragmentation functions, motivated by the SU(6) symmetric wave functions of the Λ hyperon, has been taken into account to provide results for different flavors. In addition, we have included the leading-order evolution effects for the fragmentation functions. Using the numerical results of $\tilde{H}(z)$, we have estimated the SSA $A_{UT}^{\sin\phi_S}$ in SIDIS at the kinematics of the EIC, EicC, and COMPASS. In our case we have integrated out the transverse momentum of the final state Λ. Our calculation shows that the estimated $\sin\phi_S$ asymmetry for the Λ production in SIDIS is sizable, around 0.1. The sign of the asymmetry is negative in the entire x and z regions. We also find that the inclusion of the evolution effects of $\tilde{H}$ can change the shape and size of the asymmetry in the intermediate regions of x and z. The evolution effects should be important for the interpretation of future experimental data. In conclusion, the $\sin\phi_S$ asymmetries of Λ production in SIDIS may be measured at the kinematics of the EIC, EicC, and COMPASS, which provide a feasible way to access the twist-3 collinear $\tilde{H}(z)$ of the Λ hyperon via the $\sin\phi_S$ asymmetry in which the transverse momentum of the final-state hadron is integrated out. Since the integration is performed in the whole region of transverse momentum P_{hT}, which is difficult to achieve experimentally, the approximation of the integration region and the validity of TMD factorization of the TMD structure function related to the twist-3 PDFs or FFs remain promising issues in practice.

ACKNOWLEDGMENTS

This work is partially supported by the Shandong Provincial Natural Science Foundation, China (Grant No. ZR2020QA081) and National Natural Science Foundation of China (Grants No. 11575043, No. 11905187, and No. 11847217). X. Wang is supported by the China Postdoctoral Science Foundation under Grant No. 2018M640680 and the Academic Improvement Project of Zhengzhou University.

APPENDIX: DOUBLE-l INTEGRALS

$$\int d^4l \frac{l^\mu l^\nu \delta(l^2)\delta((k-l)^2-m^2)}{((k-P_h-l)^2-m_s^2)} = \mathcal{AA}k^\mu k^\nu + \mathcal{BB}P^\mu P^\nu + \mathcal{AB}(k^\mu P^\nu + P^\mu k^\nu) + g^{\mu\nu}\mathcal{W}_1, \tag{A1}$$

where

$$\begin{aligned}
\mathcal{AA} &= -\frac{(k^2-m^2)[k^2M^2(3\mathcal{A}+\mathcal{B}) - 2(\mathcal{B}-\mathcal{A})(k\cdot P)^2 - \mathcal{B}M^2 k\cdot P]}{k^2\lambda(m_s,M)} \\
\mathcal{BB} &= -\frac{(k^2-m^2)((\mathcal{A}+3\mathcal{B})k^2 - 2\mathcal{B}k\cdot P)}{\lambda(m_s,M)} \\
\mathcal{AB} &= -\frac{(k^2-m^2)(2\mathcal{B}M^2 - (\mathcal{A}+3\mathcal{B})k\cdot P)}{\lambda(m_s,M)} \\
\mathcal{W}_1 &= -\frac{(\mathcal{A}+\mathcal{B})(k^2-m^2)}{4}.
\end{aligned}$$

Note that $4k^2M^2 - 4(k\cdot P)^2 = (4k^2M^2 - (k^2+M^2-m_s^2)^2) = -\lambda(m_s,M)$,

$$\int d^4l \frac{l^\mu l^\nu \delta(l^2)\delta((k-l)^2-m^2)}{((k-P_h-l)^2-m_s^2)(-l\cdot n_+ + i\epsilon)} = \mathcal{CC}_f k^\mu k^\nu + \mathcal{DD}_f P^\mu P^\nu + \mathcal{EE}_f n_+^\mu n_+^\nu \tag{A2}$$

$$+ \mathcal{CD}_f(k^\mu P^\nu + P^\mu k^\nu) + \mathcal{CE}_f(k^\mu n_+^\nu + n_+^\mu k^\nu) + \mathcal{DE}_f(n_+^\mu P^\nu + P^\mu n_+^\nu) + g^{\mu\nu}\mathcal{W}_2, \tag{A3}$$

where

$$\mathcal{CC}_f k^- = -\frac{2z(\mathcal{A}-\mathcal{B})k\cdot P - 2\mathcal{A}k^2 z - \mathcal{A}M_\Lambda^2 + \mathcal{B}M_\Lambda^2 z + \mathcal{C}k^-(z-1)z(k^2-m^2)}{z^2\boldsymbol{k}_T^2} \tag{A4}$$

$$\mathcal{CD}_f k^- = \frac{\mathcal{A}k^2 z - 2\mathcal{A}k^2 - 2\mathcal{B}k\cdot P + \mathcal{B}M_\Lambda^2 + \mathcal{C}k^-(z-1)(k^2-m^2)}{z^2\boldsymbol{k}_T^2} \tag{A5}$$

$$\mathcal{CE}_f k^- k^- = -\frac{2(k\cdot P(\mathcal{B}(k^2z^2+M_\Lambda^2(z-1)) - \mathcal{A}k^2z^2) + k^2(\mathcal{A}(k^2z^2+M_\Lambda^2(z-1)) - \mathcal{B}M_\Lambda^2 z^2))}{2z^3\boldsymbol{k}_T^2} \tag{A6}$$

$$-\frac{\mathcal{C}k^-(k^2-m^2)(k^2z^2 - 2z^2 k\cdot P + M_\Lambda^2(2z-1))}{2z^3\boldsymbol{k}_T^2}. \tag{A7}$$

[1] K. Abe *et al.* (Belle Collaboration), Phys. Rev. Lett. **96**, 232002 (2006).
[2] R. Seidl *et al.* (Belle Collaboration), Phys. Rev. D **78**, 032011 (2008); **86**, 039905(E) (2012).
[3] J. P. Lees *et al.* (*BABAR* Collaboration), Phys. Rev. D **90**, 052003 (2014).
[4] M. Ablikim *et al.* (BESIII Collaboration), Phys. Rev. Lett. **116**, 042001 (2016).
[5] Y. Guan *et al.* (Belle Collaboration), Phys. Rev. Lett. **122**, 042001 (2019).
[6] A. Airapetian *et al.*, Phys. Rev. Lett. **94**, 012002 (2005).
[7] A. Airapetian *et al.*, Phys. Lett. B **693**, 11 (2010).
[8] X. Qian *et al.* (Jefferson Lab Hall A Collaboration), Phys. Rev. Lett. **107**, 072003 (2011).
[9] C. Adolph *et al.* (COMPASS Collaboration), Phys. Lett. B **744**, 250 (2015).
[10] A. Lesnik *et al.*, Phys. Rev. Lett. **35**, 770 (1975).
[11] G. Bunce *et al.*, Phys. Rev. Lett. **36**, 1113 (1976).
[12] J. Adams *et al.* (STAR Collaboration), Phys. Rev. Lett. **92**, 171801 (2004).
[13] B. I. Abelev *et al.* (STAR Collaboration), Phys. Rev. Lett. **101**, 222001 (2008).
[14] J. H. Lee, and F. Videbæk (BRAHMS Collaboration), AIP Conf. Proc. **915**, 533 (2007).
[15] L. Adamczyk *et al.* (STAR Collaboration), Phys. Rev. D **86**, 051101 (2012).
[16] J. C. Collins, Nucl. Phys. **B396**, 161 (1993).
[17] D. Boer, R. Jakob, and P. J. Mulders, Phys. Lett. B **424**, 143 (1998).
[18] D. de Florian, M. Stratmann, and W. Vogelsang, Phys. Rev. D **57**, 5811 (1998).
[19] C. Boros and Z. t. Liang, Phys. Rev. D **57**, 4491 (1998).
[20] B. Q. Ma and J. Soffer, Phys. Rev. Lett. **82**, 2250 (1999).
[21] B. Q. Ma, I. Schmidt, and J. J. Yang, Phys. Lett. B **477**, 107 (2000).
[22] M. Anselmino, D. Boer, U. D'Alesio, and F. Murgia, Phys. Rev. D **63**, 054029 (2001).
[23] A. Bacchetta, R. Kundu, A. Metz, and P. J. Mulders, Phys. Lett. B **506**, 155 (2001).
[24] A. Bacchetta, R. Kundu, A. Metz, and P. J. Mulders, Phys. Rev. D **65**, 094021 (2002).
[25] L. P. Gamberg, G. R. Goldstein, and K. A. Oganessyan, Phys. Rev. D **68**, 051501 (2003).
[26] A. Bacchetta, A. Metz, and J. J. Yang, Phys. Lett. B **574**, 225 (2003).
[27] D. Amrath, A. Bacchetta, and A. Metz, Phys. Rev. D **71**, 114018 (2005).
[28] Q. h. Xu, Z. t. Liang, and E. Sichtermann, Phys. Rev. D **73**, 077503 (2006).
[29] A. Bacchetta, L. P. Gamberg, G. R. Goldstein, and A. Mukherjee, Phys. Lett. B **659**, 234 (2008).
[30] B. Zhang, Z. Lu, B. Q. Ma, and I. Schmidt, Phys. Rev. D **78**, 034035 (2008).
[31] M. Anselmino, M. Boglione, U. D'Alesio, S. Melis, F. Murgia, and A. Prokudin, Phys. Rev. D **87**, 094019 (2013).
[32] Z. B. Kang, A. Prokudin, P. Sun, and F. Yuan, Phys. Rev. D **91**, 071501 (2015).
[33] Z. B. Kang, Phys. Rev. D **83**, 036006 (2011).
[34] K. Kanazawa and Y. Koike, Phys. Rev. D **88**, 074022 (2013).
[35] L. Gamberg, Z. B. Kang, D. Pitonyak, M. Schlegel, and S. Yoshida, J. High Energy Phys. 01 (2019) 111.
[36] S. Y. Wei, K. b. Chen, Y. k. Song, and Z. t. Liang, Phys. Rev. D **91**, 034015 (2015).

[37] U. D'Alesio, F. Murgia, and M. Zaccheddu, Phys. Rev. D **102**, 054001 (2020).
[38] D. Callos, Z. B. Kang, and J. Terry, Phys. Rev. D **102**, 096007 (2020).
[39] A. Metz, Phys. Lett. B **549**, 139 (2002).
[40] J. C. Collins and A. Metz, Phys. Rev. Lett. **93**, 252001 (2004).
[41] D. Boer, P. J. Mulders, and F. Pijlman, Nucl. Phys. **B667**, 201 (2003).
[42] F. Yuan, Phys. Rev. Lett. **100**, 032003 (2008); Phys. Rev. D **77**, 074019 (2008).
[43] L. P. Gamberg, A. Mukherjee, and P. J. Mulders, Phys. Rev. D **77**, 114026 (2008); **83**, 071503(E) (2011).
[44] S. Meissner and A. Metz, Phys. Rev. Lett. **102**, 172003 (2009).
[45] J. w. Qiu and G. F. Sterman, Phys. Rev. D **59**, 014004 (1998).
[46] H. Eguchi, Y. Koike, and K. Tanaka, Nucl. Phys. **B752**, 1 (2006).
[47] Z. B. Kang, F. Yuan, and J. Zhou, Phys. Lett. B **691**, 243 (2010).
[48] K. Kanazawa, Y. Koike, A. Metz, and D. Pitonyak, Phys. Rev. D **89**, 111501 (2014).
[49] Y. Koike, A. Metz, D. Pitonyak, K. Yabe, and S. Yoshida, Phys. Rev. D **95**, 114013 (2017).
[50] K. Kanazawa, A. Metz, D. Pitonyak, and M. Schlegel, Phys. Lett. B **742**, 340 (2015).
[51] A. V. Efremov and O. V. Teryaev, Yad. Fiz. **36**, 242 (1982) [Sov. J. Nucl. Phys. **36**, 140 (1982)], https://inspirehep.net/literature/167526.
[52] A. V. Efremov and O. V. Teryaev, Phys. Lett. **150B**, 383 (1985).
[53] J. w. Qiu and G. F. Sterman, Nucl. Phys. **B378**, 52 (1992).
[54] Z. B. Kang, J. W. Qiu, W. Vogelsang, and F. Yuan, Phys. Rev. D **83**, 094001 (2011).
[55] A. Metz and D. Pitonyak, Phys. Lett. B **723**, 365 (2013); **762**, 549(E) (2016).
[56] A. Bacchetta, M. Diehl, K. Goeke, A. Metz, P. J. Mulders, and M. Schlegel, J. High Energy Phys. 02 (2007) 093.
[57] Z. Lu and I. Schmidt, Phys. Lett. B **747**, 357 (2015).
[58] X. Wang and Z. Lu, Phys. Rev. D **93**, 074009 (2016).
[59] Y. Yang, Z. Lu, and I. Schmidt, Phys. Rev. D **96**, 034010 (2017).
[60] X. Wang, Y. Yang, and Z. Lu, Phys. Rev. D **97**, 114015 (2018).
[61] L. P. Gamberg, D. S. Hwang, A. Metz, and M. Schlegel, Phys. Lett. B **639**, 508 (2006).
[62] X. d. Ji and F. Yuan, Phys. Lett. B **543**, 66 (2002).
[63] A. V. Belitsky, X. Ji, and F. Yuan, Nucl. Phys. **B656**, 165 (2003).
[64] M. Nzar and P. Hoodbhoy, Phys. Rev. D **51**, 32 (1995).
[65] R. Jakob, P. J. Mulders, and J. Rodrigues, Nucl. Phys. **A626**, 937 (1997).
[66] Y. Yang, Z. Lu, and I. Schmidt, Phys. Lett. B **761**, 333 (2016).
[67] R. Van Royen and V. F. Weisskopf, Nuovo Cimento A **50**, 617 (1967); **51**, 583(E) (1967).
[68] R. Jakob, P. Kroll, M. Schurmann, and W. Schweiger, Z. Phys. A **347**, 109 (1993).
[69] M. Gluck, E. Reya, and A. Vogt, Z. Phys. C **67**, 433 (1995).
[70] M. Gluck, E. Reya, M. Stratmann, and W. Vogelsang, Phys. Rev. D **53**, 4775 (1996).
[71] M. Gluck, E. Reya, and A. Vogt, Phys. Rev. D **48**, 116 (1993); **51**, 1427(E) (1995).
[72] K. Ackerstaff *et al.* (OPAL Collaboration), Eur. Phys. J. C **2**, 39 (1998).
[73] J. P. Ma and G. P. Zhang, Phys. Lett. B **772**, 559 (2017).
[74] Z. B. Kang, A. Prokudin, P. Sun, and F. Yuan, Phys. Rev. D **93**, 014009 (2016).
[75] M. Botje, Comput. Phys. Commun. **182**, 490 (2011).
[76] D. Boer and P. J. Mulders, Phys. Rev. D **57**, 5780 (1998).
[77] H. L. Lai, M. Guzzi, J. Huston, Z. Li, P. M. Nadolsky, J. Pumplin, and C. P. Yuan, Phys. Rev. D **82**, 074024 (2010).
[78] D. de Florian, R. Sassot, M. Stratmann, and W. Vogelsang, Phys. Rev. Lett. **101**, 072001 (2008).
[79] A. Accardi *et al.*, Eur. Phys. J. A **52**, 268 (2016).
[80] X. Cao, L. Chang, N. B. Chang *et al.*, Nucl. Tech. (Chinese Version) **43**, 020001 (2020).
[81] D. P. Anderle *et al.*, arXiv:2102.09222.
[82] M. G. Alekseev *et al.* (COMPASS Collaboration), Phys. Lett. B **692**, 240 (2010).
[83] Z. Lu, B. Q. Ma, and J. Zhu, Phys. Rev. D **84**, 074036 (2011).
[84] S. C. Xue, X. Wang, D. M. Li, and Z. Lu, Eur. Phys. J. C **80**, 685 (2020).
[85] A. Bacchetta, F. Conti, and M. Radici, Phys. Rev. D **78**, 074010 (2008).